An Empirical Investigation on the Effect of Oxygen Vacancy in ZrO_2 Thin Film on the Frequency-Dependent Capacitance Degradation in the Metal–Insulator–Metal Capacitor

Dong Hee Han, Seungwoo Lee, Ji Hyeon Hwang, Youngjin Kim, Marceline Bonvalot, Christophe Vallée, Patrice Gonon, and Woojin Jeon

***Abstract*— The operation speed of dynamic random access memory devices has been increasing with respect to the evolution of electronic devices. This in turn has induced a decrease in the allowed time for the operation. Therefore, the effective capacitance degradation in which the capacitance gradually decreases with increasing frequency of applied ac voltage is a severe concern for decreasing capacitance during fast operation, in addition to inducing reliability degradation. Hence, in this article, the origin of capacitance degradation depending on operation frequency, also called "frequency dependence" of the capacitance, was revealed. By performing dc and ac nonlinearity analyses, the effect of defects, especially oxygen vacancies, on the electrical properties of metal-insulator-metal (MIM) capacitors was investigated. Eventually, the mechanism of frequency dependence related to oxygen vacancy in the insulator of the MIM capacitor was identified.**

***Index Terms*— Capacitors, dielectrics, dynamic random access memory (DRAM) chips, frequency response, metal-insulator structures.**

Manuscript received July 23, 2021; revised August 12, 2021; accepted August 31, 2021. Date of publication September 14, 2021; date of current version October 22, 2021. This work was supported in part by the Technology Innovation Program under Grant 20003555 and Grant 20016813, and in part by the Korea Institute of Energy Technology Evaluation and Planning (KETEP) funded by the Ministry of Trade, Industry and Energy (MOTIE, Korea) under Grant 20201520300140 (Development of Advanced Functional Material With C-14 From PHWR Waste). The work of Woojin Jeon was supported by SK Hynix. The review of this article was arranged by Editor J.-S. Park. *(Corresponding author: Woojin Jeon.)*

Dong Hee Han, Seungwoo Lee, and Woojin Jeon are with the Department of Advanced Materials Engineering for Information and Electronics, Kyung Hee University, Yongin, Gyeonggi 17104, South Korea, and also with the Integrated Education Institute for Frontier Science and Technology (BK21 Four), Kyung Hee University, Yongin, Gyeonggi 17104, South Korea (e-mail: woojin.jeon@khu.ac.kr).

Ji Hyeon Hwang is with the Department of Advanced Materials Engineering for Information and Electronics, Kyung Hee University, Yongin, Gyeonggi 17104, South Korea, also with the Integrated Education Institute for Frontier Science and Technology (BK21 Four), Kyung Hee University, Yongin, Gyeonggi 17104, South Korea, and also with the Soft Hybrid Materials Research Center, Korea Institute of Science and Technology, Seoul 02792, South Korea.

Youngjin Kim is with the Soft Hybrid Materials Research Center, Korea Institute of Science and Technology, Seoul 02792, South Korea.

Marceline Bonvalot and Patrice Gonon are with the Microelectronics Technology Laboratory (LTM), National Center for Scientific Research (CNRS), Grenoble Alpes University (UGA), 75016 Paris, France, and also with CEA-LETI, Minatec Campus, 38054 Grenoble, France.

Christophe Vallée is with Grenoble Alpes University (UGA), 38000 Grenoble, France, and also with CNSE, SUNY POLY, Albany, NY 12203 USA.

Color versions of one or more figures in this article are available at https://doi.org/10.1109/TED.2021.3110837.

Digital Object Identifier 10.1109/TED.2021.3110837

I. INTRODUCTION

ZrO_2 is one of the most eminent high-dielectric-constant (k) materials for capacitor dielectric applications, especially in dynamic random access memory (DRAM) [1]–[6]. A metal–insulator–metal (MIM) structured capacitor consisting of TiN as the top and bottom electrodes (BEs) and a ZrO_2-based dielectric as the insulator has been employed in DRAM capacitors over a decade [2]–[6], because ZrO_2 can satisfy requirements such as compatibility of the deposition process, ease of obtaining a relatively high-k value, and low leakage current level with thin physical thickness. However, one of the limitations of the TiN/ZrO_2-based MIM capacitor in fulfilling the requirements of next-generation DRAM is that the increased operation speed induces a decrease in the time allowed for charging the capacitor [7], making stable operation at high frequency one of the newly required parameters. As charging the capacitor is a time-consuming process depending on the polarization mechanisms, the capacitance of the capacitor has a frequency dependence (decreasing capacitance with increasing frequency) [8], [9]. Similarly, the capacitance of the TiN/ZrO_2-based MIM capacitor exhibits severe capacitance degradation with increased frequency: the relative capacitance is 0.91 at 100 kHz, compared to the value at 1 kHz [9]. Although this "frequency dependence of capacitance" becomes more serious with the advance of DRAM technology, research on this topic has rarely been conducted.

In this study, the mechanism of frequency dependence of the capacitance in the TiN/ZrO_2/TiN MIM structure was investigated. Oxygen vacancies (V_O) were formed deliberately to control the concentration and gradient of the ZrO_2 thin film. The examination of dc and ac nonlinearity behaviors using the capacitance–voltage (C–V) measurements in various ZrO_2

0018-9383 © 2021 IEEE. Personal use is permitted, but republication/redistribution requires IEEE permission.
See https://www.ieee.org/publications/rights/index.html for more information.

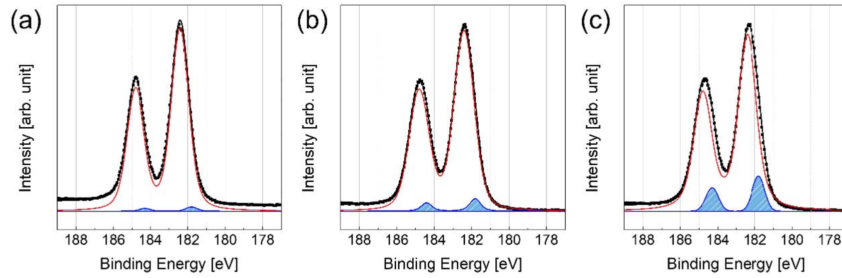

Fig. 1. Zr 3d XPS profiles of (a) ZrO_2, (b) ZAZ, and (c) ZTZ thin films.

thin films with different V_O concentrations was performed to thoroughly investigate the frequency dependence, based on the V_O at the bulk or interface region of the TiN/ZrO_2-based MIM capacitor.

II. Experimental Procedures

Pristine ZrO_2, Al-doped ZrO_2 (ZAZ), and Ti-doped ZrO_2 (ZTZ) thin films were used as dielectric layers in MIM capacitors. The BE consisted of sputtered TiN (200 nm)/SiO_2/Si stacks. The dielectric layers were deposited on the BEs through thermal atomic layer deposition (ALD, Nexus Mini 4.5, Nexusbe Company, Ltd.), with tetrakis-ethylmethylamino-zirconium ($Zr[N(CH_3)(C_2H_5)]_4$, TEMAZ), trimethylaluminum ($Al(CH_3)_3$, TMA), and titanium tetraisopropoxide ($Ti(O(C_3H_7))_4$, TTIP) for the Zr, Al, and Ti precursors, respectively. O_3 was used as the oxygen source at a concentration of 200 g/m^3. The canisters of TEMAZ, TMA, and TTIP were maintained at 60 °C, room temperature, and 40 °C to acquire the appropriate vapor pressures of each precursor, respectively.

The deposition temperature was set to 270 °C for all the dielectrics. The doping sequences of the Al and Ti in the ZrO_2 dielectrics were performed using ALD super-cycles, which consisted of ALD subcycles of ZrO_2, Al_2O_3, and TiO_2 with different cycle ratios to clarify the identical doping thickness of 0.5 nm of Al_2O_3 and TiO_2 in the ZrO_2 films. The doping positions of Al and Ti were defined by dividing the total number of ZrO_2 ALD cycles by 6 and depositing 0.1-nm-thick Al_2O_3 and TiO_2 between them. The total thicknesses of all samples were fixed to 10 nm.

The film thickness was determined by calculating the layer density, which was measured via X-ray fluorescence spectroscopy (XRF, ARL Quant'X, Thermo Scientific), and correlated with transmission electron microscopy (TEM, Tecnai Osiris, FEI) measurements. The thickness of the Al_2O_3 layer was measured using spectroscopic ellipsometry (ESM-300, J. A. Woollam). Postdeposition annealing was performed at 600 °C for 30 s under N_2 atmosphere using a rapid thermal process to enhance the electrical properties. An MIM capacitor was fabricated with a top electrode (TE) to measure the electrical properties. This consisted of 10-nm-thick TiN and 50-nm-thick Pt film that was deposited via dc sputtering, defined by a metal shadow mask with a 300 μm diameter hole.

The chemical state of the interface between the dielectric and BE layers was investigated via X-ray photoelectron spectroscopy (XPS, MXP10, ThermoFisher Scientific). The electrical properties were evaluated by measuring the capacitance versus voltage and the capacitance versus frequency characteristics, using an *LCR* meter (Agilent 4284). During the measurement of the electrical characteristics, a positive or negative voltage was applied to the TE, while the BE was grounded.

III. Results and Discussion

Initially, V_O formation in the ZrO_2 thin film was investigated by introducing the dopant. Al_2O_3 and TiO_2 were employed as dopants, by constituting the super-cycle with the ZrO_2 ALD deposition process. The V_O concentration in the ZrO_2 thin films was quantified using XPS surface analysis. The peak position was recalibrated based on the C–C bond peak position (C 1s peak), considering a binding energy of 284.8 eV. The Zr 3d core level in the XPS profiles was composed of Zr $3d_{5/2}$ peaks centered at binding energies of 182.3 and 181.8 eV, which corresponded to the energies of ZrO_2 and ZrO_{2-x} ($x < 1$), respectively (Fig. 1) [9]–[11]. The lower binding energy of the Zr 3d peak from ZrO_{2-x} indicates the less oxidized Zr ion; successively, the increased ratio of ZrO_{2-x} implied an increased V_O concentration in the ZrO_2 thin film [11]–[13]. In the case of the pristine ZrO_2 thin film, the ZrO_{2-x} ratio was 1.5%. The ZrO_{2-x} ratio increased to 4.1% in the ZAZ thin film, owing to the introduced aliovalent Al^{3+} ion. In the case of the ZTZ thin film, however, the ZrO_{2-x} ratio significantly increased to 10.4%. This V_O formation in the ZrO_2 thin film through Ti doping was presumably affected by the lattice relaxation in ZrO_2 because of the smaller ionic radius of substitutional Ti dopants [14]. Consequently, ZrO_2 thin films with various V_O concentrations were fabricated by introducing Al and Ti dopants.

The dc nonlinearity behavior in the C–V curves of the MIM capacitors, consisting of ZrO_2, ZAZ, and ZTZ was investigated. Fig. 2(a) shows the dc-bias-dependent (V_{dc}) relative capacitance (C/C_0, where C_0 is the capacitance at zero dc bias) curves of the MIM capacitors, measured at 303 K. The C/C_0–V_{dc} curve of pristine ZrO_2 exhibited the typical shape of the MIM capacitor with TiN/ZrO_2/TiN, increasing the C/C_0 with increasing V_{dc}, as well as asymmetry in the polarity of V_{dc}. The calculated quadratic voltage coefficient of the capacitance (α), which was derived from the expression $C/C_0 = 1 + \beta V + \alpha V^2$, where β is the linear voltage coefficient of the capacitance, was 0.431×10^{-2} V^{-2}, and

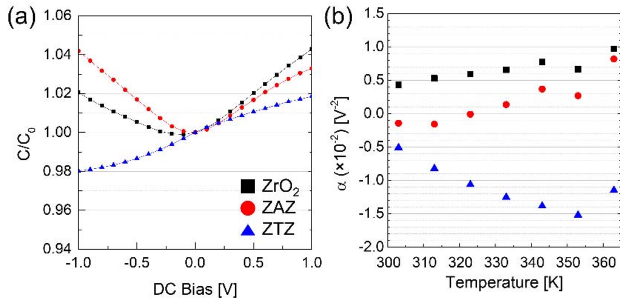

Fig. 2. (a) C/C_0–V_{dc} curves of MIM capacitors with various thin films. (b) Extracted α values from the C/C_0–V_{dc} curves in various temperatures.

TABLE I

α VALUES EXTRACTED FROM THE C/C_0–V_{dc} CURVE OF MIM CAPACITORS IN VARIOUS TEMPERATURES

(CUR^{-2}) [V^{-2}]	303 K	313 K	323 K	333 K	343 K	353 K	363 K
ZrO_2	0.431	0.53	0.593	0.655	0.772	0.665	0.969
ZAZ	-0.145	-0.16	-0.010	0.135	0.366	0.268	0.819
ZTZ	-0.511	-0.823	-1.064	-1.253	-1.385	-1.521	-1.149

increased with increasing temperature, eventually reaching 0.969×10^{-2} V^{-2} at 363 K. This dc nonlinearity indicated the contribution of V_O, at the interface of the TiN electrode and ZrO_2 insulator, to the capacitance [15]–[17]. The V_O at the interface would contribute additional polarization by trapping and detrapping electrons through hopping through applied ac bias, which was called "electrode polarization" [8]. When the applied V_{dc} increased, the driving force on the hopping process increased, resulting in an increase in the relative capacitance (C/C_0). Therefore, dc nonlinearity implied the V_O concentration at the interface. Moreover, the asymmetry indicated different V_O concentrations at the interfaces of the TiN BE/ZrO_2 and ZrO_2/TiN TE [9], [11]. More severe dc nonlinearity at the positive V_{dc} (electron injection from the BE) than the negative V_{dc} (electron injection from the TE) denoted a relatively high V_O concentration at the interface of TiN BE/ZrO_2. In the case of the ZAZ thin film, the α value significantly decreased compared to that of the ZrO_2 thin film (Table I). The α value was almost 0 at 303–323 K. Moreover, asymmetry was not observed. The C/C_0–V_{dc} behavior of ZAZ implied that the contribution of V_O at the interface was reduced by introducing the Al dopant. The C/C_0–V_{dc} curve of ZTZ exhibited a completely different shape from the others. The α value was lower than 0 at all examined temperatures. Moreover, the capacitance decreased with increasing V_{dc} over a temperature of 333 K (data not shown). This opposing behavior, which was generally observed in the MIM capacitor with the insulator containing relatively poor leakage current property [18]–[22], originated from the severely degraded leakage current property of the ZTZ thin film. Owing to the leakage current with respect to V_{dc}, the C/C_0–V_{dc} curve of ZTZ had the opposite trend. In fact, the dielectric loss increased with increasing V_{dc}. Therefore, it was difficult to determine the contribution of V_O in the ZTZ thin film to the C–V characteristics from the dc nonlinearity investigation.

Furthermore, the ac nonlinearity of the MIM capacitors with ZrO_2, ZAZ, and ZTZ was investigated. In the general C–V measurement, an ac bias is imposed on V_{dc} to respond to the charging of electrons on the electrode. At the same time, charged particles in the insulator, such as electrons trapped in a trap, or charged defect, would respond to the electric field (E-field) induced by the ac bias. The ac bias consists of the level and frequency. As the ac level (V_{ac}) increased, the driving force on the response of electrons regarding the E-field will be increased. As the ac frequency increased, the magnitude

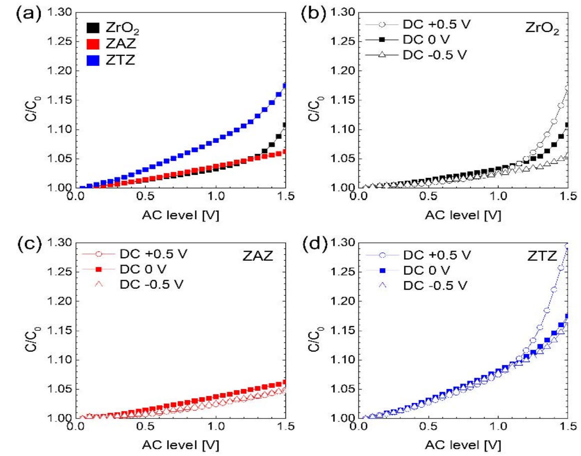

Fig. 3. (a) C/C_0–V_{ac} curves of MIM capacitors with various thin films. C/C_0–V_{ac} curves with varied V_{dc} for (b) ZrO_2, (c) ZAZ, and (d) ZTZ, respectively.

of the response will be decreased [9]. In this regard, the ac nonlinearity in the C/C_0–V_{ac} (C_0 is the capacitance at zero V_{ac}, in this case) curve indicates the relative V_O concentration in the bulk region of the insulator [15]–[17]. As shown in Fig. 3(a), the MIM capacitor with ZTZ thin film exhibited relatively high ac nonlinearity behavior compared to ZAZ and ZrO_2. This severe nonlinearity in the ZTZ thin film was consistent with the V_O concentration in the XPS analysis. Moreover, the V_O concentration gradient in the insulator was estimated by applying V_{dc} during the C/C_0–V_{ac} measurements. In the case of the ZAZ thin film, no difference in the C/C_0–V_{ac} curves with varying V_{dc} was observed, implying that the ZAZ thin film had negligible V_O concentration. Therefore, no characteristic behavior due to the V_O contribution was observed in dc [Fig. 2(a)] or ac nonlinearity [Fig. 3(c)]. In the case of the ZrO_2 thin film, a difference in the ac nonlinearity was observed depending on the V_{dc} polarity. With positive V_{dc}, where the positively charged V_O tended to accumulate adjacent to the BE, the ac nonlinearity was relatively high compared to V_{dc} of 0 and −0.5 V. The ac nonlinearity decreased gradually with decreased V_{dc}; eventually, the lowest ac nonlinearity was observed with V_{dc} of −0.5 V, where the V_O near the TE would react to the applied ac bias. This trend was well corroborated by the asymmetry observed in the C/C_0–V_{dc} curve of the ZrO_2 thin film [Fig. 2(a)]. In other words, the V_O distribution in the insulator could be assessed by varying V_{dc} during C/C_0–V_{ac} measurements were performed. Using this

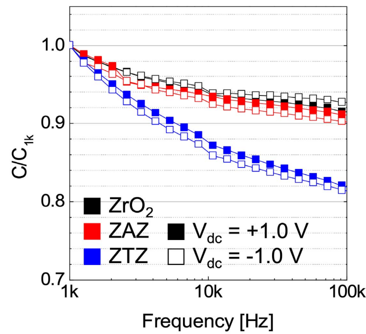

Fig. 4. C/C_{1k}-frequency curves for ZrO_2, ZAZ, and ZTZ thin films with varied V_{dc}.

measurement technique, the V_O distribution in the ZTZ thin film was investigated. However, it was difficult to distinguish V_O distribution from the asymmetry in the C/C_0–V_{dc} curve, due to significantly high leakage current in the ZTZ thin film. The fact that the ac nonlinearity with V_{dc} of +0.5 V was relatively higher than that of V_{dc} of 0 and −0.5 V inferred that the ZTZ thin film also had a relatively higher V_O concentration at the area adjacent to the BE.

From the dc and ac nonlinearity evaluation results for ZrO_2, ZAZ, and ZTZ thin films, it could be confirmed that each thin film had its own distinct characteristics, in relation to the V_O distribution. The ZrO_2 thin film had a gradient of V_O with relatively high concentration at the interface with the BE, and gradually decreased toward the interface with TE. This was consistent with the previous results on V_O formation by the interaction of the TiN TE and ZrO_2 during the ZrO_2 ALD deposition process. In the case of the ZAZ thin film, V_O-induced dc or ac nonlinearity was not observed, even though the XPS profile indicated V_O formation by introducing the Al dopant. In a previous study, it was suggested that V_O formation by doping with an aliovalent dopant does not induce any degradation in the electrical properties related to V_O [4], [6], [11], [23]. Consequently, the V_O in the ZAZ thin film, introduced by the Al dopant in ZrO_2, did not contribute to the dc and ac nonlinearity. However, Ti doping in the ZTZ thin film resulted in severe dc and ac nonlinearity behaviors. In turn, the V_O distribution characteristics of each film were summarized as follows: the ZAZ thin film had negligible V_O concentration, ZrO_2 thin film had considerable V_O concentration in the limited area at the interface with the BE, and the ZTZ thin film had significant V_O concentration at the interface with the BE, as well as in the bulk region.

Finally, the frequency dependence behaviors were examined in the MIM capacitors with ZrO_2, ZAZ, and ZTZ as insulators (Fig. 4). As the frequency of the ac bias was increased, C/C_{1k} (C_{1k} is the capacitance at an ac frequency of 1 kHz) decreased in all MIM capacitors. However, the magnitude of the decrease changed depending on the insulator. In the case of ZTZ, C/C_{1k} at a frequency of 100 kHz was significantly lower than that of ZrO_2 and ZAZ. Moreover, it was emphasized that the frequency dependence of ZrO_2 and ZAZ did not exhibit notable differences, even though these insulators had different dc nonlinearity properties. Meanwhile, no dependency was observed for V_{dc} during C/C_{1k}-frequency curve measurement. The above results were observed for C/C_{1k}-frequency curves, and the relationship between the frequency dependence and V_O in the insulator was derived. Initially, V_O at the interface did not influence the frequency dependence. If the V_O at the interface governed the frequency dependence, C/C_{1k}-frequency curves would exhibit a difference in V_O concentration at the interface (ZrO_2 and ZAZ in this case), or a difference in the polarity of V_{dc}. However, the insulators had a significant V_O concentration difference between the two interfaces (ZTZ and ZrO_2 in this case), as shown in the ac nonlinearity examinations. This significant V_O concentration could not induce any difference in C/C_{1k}-frequency curve, depending on the polarity of V_{dc}. In contrast to V_O at the interface, V_O at the bulk induced severe frequency dependence. It was revealed that only the ZTZ thin film had a considerable V_O concentration in the bulk region from the ac nonlinearity. In C/C_{1k}-frequency curves, only the ZTZ thin film exhibited notable frequency dependence. Consequently, it could be concluded that the frequency dependence in the MIM capacitor related to V_O was strongly dependent on the V_O in the bulk region of the insulator, rather than the V_O at the interface.

IV. Conclusion

The frequency dependence of the TiN/ZrO_2/TiN structured capacitor with respect to V_O was investigated. ZrO_2 thin films with various V_O concentrations were varied by Al_2O_3 and TiO_2 doping. From the dc and ac nonlinearity results, a distinctive V_O distribution in the ZrO_2 thin films was observed. Relatively high dc nonlinearity and dc bias polarity dependence on the ac nonlinearity confirmed V_O formation at the interface of TiN BE and ZrO_2 during the ZrO_2 ALD process. TiO_2 doping in ZrO_2 thin films also induced V_O defects in the bulk region. Moreover, employing the Al_2O_3 dopant suppressed V_O at the interface, influencing the electrical properties and C–V measurement in this work. These differences in the V_O of the insulators strongly affected the C/C_{1k}-frequency property. The frequency dependence of the MIM capacitor was only governed by V_O in the bulk region, rather than those at the interface. Accordingly, the origin of the capacitance degradation in the high-frequency operation of DRAM was clearly identified.

Acknowledgment

The authors would like to thank the SK Trichem Company, Ltd., for supporting this work as a precursor supplier.

References

[1] W. Lee *et al.*, "Electrical properties of $ZrO_2/Al_2O_3/ZrO_2$-based capacitors with TiN, Ru, and TiN/Ru top electrode materials," *Phys. Status Solidi (RRL)-Rapid Res. Lett.*, vol. 12, no. 10, Oct. 2018, Art. no. 1800356, doi: 10.1002/PSSR.201800356.

[2] D.-S. Kil *et al.*, "Development of new TiN/$ZrO_2/Al_2O_3/ZrO_2$/TiN capacitors extendable to 45 nm generation DRAMs replacing HfO_2 based dielectrics," in *Symp. VLSI Technol., Dig. Tech. Papers.*, Jun. 2006, pp. 38–39, doi: 10.1109/VLSIT.2006.1705205.

[3] S. Y. Lee, J. Chang, Y. Kim, H. Lim, H. Jeon, and H. Seo, "Depth resolved band alignments of ultrathin TiN/ZrO_2 and TiN/ZrO_2-Al_2O_3-ZrO_2 dynamic random access memory capacitors," *Appl. Phys. Lett.*, vol. 105, no. 20, Nov. 2014, Art. no. 201603, doi: 10.1063/1.4902244.

[4] H. J. Cho *et al.*, "New TIT capacitor with $ZrO_2/Al_2O_3/ZrO_2$ dielectrics for 60 nm and below DRAMs," *Solid-State Electron.*, vol. 51, nos. 11–12, pp. 1529–1533, Nov. 2007, doi: 10.1016/J.SSE.2007.09.030.

[5] Y. Kim *et al.*, "Effects of interfacial layer on characteristics of TiN/ZrO_2 structures," *J. Nanosci. Nanotechnol.*, vol. 11, no. 9, pp. 8309–8312, Sep. 2011, doi: 10.1166/JNN.2011.5043.

[6] W. Weinreich *et al.*, "Detailed leakage current analysis of metal-insulator-metal capacitors with ZrO_2, $ZrO_2/SiO_2/ZrO_2$, and $ZrO_2/Al_2O_3/ZrO_2$ as dielectric and TiN electrodes," *J. Vac. Sci. Technol. B, Nanotechnol. Microelectron., Mater., Process., Meas., Phenomena*, vol. 31, no. 1, Jan. 2013, Art. no. 01A109, doi: 10.1116/1.4768791.

[7] M. Kiyotoshi *et al.*, "Control of two types of dielectric relaxation current for Ta_2O_5 metal-insulator-metal capacitors," *Jpn. J. Appl. Phys.*, vol. 42, no. 4S, p. 1943, Apr. 2003, doi: 10.1143/JJAP.42.1943.

[8] A. Akshaykranth and R. Karthik, "Frequency dependence of capacitance modeling in metal-insulator-metal capacitors," in *Proc. Int. Conf. Electron., Commun. Aerosp. Technol. (ICECA)*, Apr. 2017, pp. 234–236, doi: 10.1109/ICECA.2017.8212804.

[9] W. Jeon, Y. Kim, C. H. An, C. S. Hwang, P. Gonon, and C. Vallée, "Demonstrating the ultrathin metal-insulator-metal diode using $TiN/ZrO_2–Al_2O_3–ZrO_2$ stack by employing RuO_2 top electrode," *IEEE Trans. Electron. Devices*, vol. 65, no. 2, pp. 660–666, Feb. 2018, doi: 10.1109/TED.2017.2785120.

[10] W. Weinreich *et al.*, "Impact of interface variations on $J–V$ and $C–V$ polarity asymmetry of MIM capacitors with amorphous and crystalline $Zr_{(1-x)}Al_xO_2$ films," *Microelectron. Eng.*, vol. 86, nos. 7–9, pp. 1826–1829, Jul. 2009, doi: 10.1016/J.MEE.2009.03.070.

[11] C. H. An *et al.*, "Controlling the electrical characteristics of $ZrO_2/Al_2O_3/ZrO_2$ capacitors by adopting a Ru top electrode grown via atomic layer deposition," *Phys. Status Solidi (RRL)-Rapid Res. Lett.*, vol. 13, no. 3, Mar. 2019, Art. no. 1800454, doi: 10.1002/PSSR.201800454.

[12] A. Sinhamahapatra, J.-P. Jeon, J. Kang, B. Han, and J.-S. Yu, "Oxygen-deficient zirconia (ZrO_{2-x}): A new material for solar light absorption," *Sci. Rep.*, vol. 6, no. 1, Jun. 2016, Art. no. 27218, doi: 10.1038/SREP27218.

[13] S. Y. Lee *et al.*, "Investigation of ultrathin $Pt/ZrO_2–Al_2O_3–ZrO_2/TiN$ DRAM capacitors Schottky barrier height by internal photoemission spectroscopy," *Current Appl. Phys.*, vol. 17, no. 2, pp. 267–271, Feb. 2017, doi: 10.1016/j.CAP.2016.12.004.

[14] H. Zhang *et al.*, "Effects of ionic doping on the behaviors of oxygen vacancies in HfO_2 and ZrO_2: A first principles study," in *Proc. Int. Conf. Simulation Semiconductor Process. Devices (SISPAD)*, Sep. 2009, pp. 1–4, doi: 10.1109/SISPAD.2009.5290225.

[15] O. Khaldi *et al.*, "Differences between direct current and alternating current capacitance nonlinearities in high-k dielectrics and their relation to hopping conduction," *J. Appl. Phys.*, vol. 116, no. 8, Aug. 2014, Art. no. 084104, doi: 10.1063/1.4893583.

[16] P. Gonon and C. Vallée, "Understanding capacitance-voltage nonlinearities in microelectronic metal-insulator-metal (MIM) capacitors," in *Proc. IEEE 11th Int. Conf. Properties Appl. Dielectr. Mater. (ICPADM)*, Jul. 2015, pp. 636–639, doi: 10.1109/ICPADM.2015.7295352.

[17] O. Khaldi, F. Jomni, P. Gonon, and C. Vallée, "AC and DC bias effect on capacitance–voltage nonlinearities in $Au/HfO_2/M$ (M = Pt, TiN, W, and AlCu) MIM capacitors: Effect of the bottom electrode material," *J. Mater. Sci. Mater. Electron.*, vol. 31, no. 21, pp. 19036–19043, Nov. 2020, doi: 10.1007/S10854-020-04440-1.

[18] S. J. Kim *et al.*, "Engineering of voltage nonlinearity in high-k MIM capacitor for analog/mixed-signal ICs," in *Symp. VLSI Technol. Dig. Tech. Paper*, Jun. 2004, pp. 218–219, doi: 10.1109/VLSIT.2004.1345489.

[19] J. Swerts *et al.*, "Leakage control in 0.4-nm EOT $Ru/SrTiO_x/Ru$ metal-insulator-metal capacitors: Process implicationss," *IEEE Electron Device Lett.*, vol. 35, no. 7, pp. 753–755, Jul. 2014, doi: 10.1109/LED.2014.2322632.

[20] W. Lee *et al.*, "Atomic layer deposition of $SrTiO_3$ films with cyclopentadienyl-based precursors for metal-insulator-metal capacitors," *Chem. Mater.*, vol. 25, no. 6, pp. 953–961, Mar. 2013, doi: 10.1021/CM304125e.

[21] S. Kupke, S. Knebel, U. Schroeder, S. Schmelzer, U. Bottger, and T. Mikolajick, "Reliability of $SrRuO_3/SrTiO_3/SrRuO_3$ stacks for DRAM applications," *IEEE Electron Device Lett.*, vol. 33, no. 12, pp. 1699–1701, Dec. 2012, doi: 10.1109/LED.2012.2219032.

[22] W. Jeon *et al.*, "Asymmetry in electrical properties of Al-doped TiO_2 film with respect to bias voltage," *Phys. Status Solidi (RRL)-Rapid Res. Lett.*, vol. 9, no. 7, pp. 410–413, Jul. 2015, doi: 10.1002/PSSR.201510146.

[23] B.-E. Park *et al.*, "Atomic layer deposition of Y-stabilized ZrO_2 for advanced DRAM capacitors," *J. Alloys Compounds*, vol. 722, pp. 307–312, Oct. 2017, doi: 10.1016/J.JALLCOM.2017.06.036.